High Preservation Potential of Paleogeographic Range Size Distributions in Deep Time

Simon A. F. Darroch,[1,*] Michelle M. Casey,[2] Gwen S. Antell,[3] Amy Sweeney,[1] and Erin E. Saupe[3]

1. Department of Earth and Environmental Sciences, Vanderbilt University, Nashville, Tennessee 37235; 2. Department of Physics, Astronomy, and Geosciences, Towson University, Towson, Maryland 21252; 3. Department of Earth Sciences, University of Oxford, South Parks Road, Oxford OX1 3AN, United Kingdom

Submitted December 2, 2019; Accepted April 20, 2020; Electronically published August 18, 2020

Online enhancements: supplemental PDF.

abstract: Reconstructing geographic range sizes from fossil data is a crucial tool in paleoecology, elucidating macroecological and macroevolutionary processes. Studies examining links between range size and extinction risk may also offer a predictive tool for identifying species most vulnerable in the "sixth mass extinction." However, the extent to which paleogeographic ranges can be recorded reliably in the fossil record is unknown. We perform simulation-based extinction experiments to examine (1) the fidelity of paleogeographic range size preservation in deep time, (2) the relative performance of different methods for reconstructing range size, and (3) the reliability of detecting patterns of extinction "selectivity" on range size. Our results suggest both that relative paleogeographic range size can be consistently reconstructed and that selectivity patterns on range size can be preserved under many extinction intensities, even when sedimentary rocks are scarce. By identifying patterns of selectivity across Earth's history, paleontologists can thus augment neontological work that aims to predict and prevent extinctions of living species. Last, we find that introducing "false extinctions" in the fossil record can produce spurious range-selectivity signals. Errors in the temporal ranges of species may pose a larger barrier to reconstructing range size–extinction risk signals than the spatial distribution of fossiliferous sediments.

Keywords: species distributions, extinction, selectivity, macroecology, macroevolution, simulations.

Introduction

The geographic ranges of species are fundamental units of biogeography, with properties (i.e., structure, organization, size, and location) controlled by a suite of factors including organismal biology, life history, niche breadth, dispersal ability, phylogenetic affinity, and historical environmental changes (Willis 1922; Anderson 1984; Brown et al. 1996; Gaston and Spicer 2001; Lester et al. 2007; Gaston 2008; Gaston and Fuller 2009). In addition to studying the present-day ranges of species, reconstructing ranges in the geological past provides a means of testing a variety of macroevolutionary and macroecological models. Geographic ranges have been linked to both speciation (Cardillo et al. 2003; Goldberg et al. 2011) and extinction (Payne and Finnegan 2007; Harnik et al. 2012; Runge et al. 2015; Saupe et al. 2015). Studies using paleo-range reconstruction have therefore illuminated the long-term processes governing the composition of local and regional biotas (e.g., Stigall 2012; Darroch et al. 2014; Darroch and Wagner 2015; Button et al. 2017; Kocsis et al. 2018) and global-scale macroecological patterns, such as the latitudinal biodiversity gradient (Tomašových et al. 2016; Kröger 2018).

The geographic range is a fundamental property of species that describes the spatial area where a species is found at an interval of time. However, ecologists and paleontologists differ in the way they measure the distribution of a taxon. Ecologists typically measure geographic ranges based on expert opinions, biological surveys, and neontological museum records on timescales of years to centuries (e.g., Brown et al. 1996). Paleontologists group fossil occurrence data within temporal bins than can range from thousands to millions of years. Paleo-ranges therefore represent a time-averaged summation of occurrences, which almost certainly amalgamate numerous geographic expansions, contractions, and shifts. Despite this mismatch, paleo-ranges represent invaluable paleobiogeographic data sets that have helped to discern the long-term processes governing modern macroecological patterns.

One area where studies in paleo-range reconstruction have become particularly prominent is in establishing links between range size and extinction risk. The size of a taxon's geographic range is thought to have regulated extinction risk during much of the geologic past (Jablonski 1986; Payne and Finnegan 2007; Harnik et al. 2012), including some mass extinction events (Jablonski 2008). Extinction has thus

* Corresponding author; email: simon.a.darroch@vanderbilt.edu.

ORCIDs: Darroch, https://orcid.org/0000-0003-1922-7136; Casey, https://orcid.org/0000-0001-9111-4182.

Am. Nat. 2020. Vol. 196, pp. 454–471.
DOI: 10.1086/710176

been "selective" with respect to geographic ranges, preferentially removing small-ranged species while large-ranged species survive. Small-ranged species are often less abundant and have narrower environmental tolerances than do larger-ranged species (Gaston 1998; Thuiller et al. 2005; Botts et al. 2013), and they may therefore be more prone to extinction during intervals of rapid environmental change (Jones et al. 2003; Jablonski 2005). Large geographic ranges may also buffer taxa from biotic or abiotic stresses affecting a specific, limited geographic area (Aberhan and Baumiller 2003; Heim and Peters 2011; Saupe et al. 2015). This relationship between range size and extinction risk has garnered attention with the recognition that global ecosystems are in rapid decline and showing signs of incipient ecosystems collapse analogous to the "big five" mass extinction events of the Phanerozoic (Barnosky et al. 2011; Hull et al. 2015). Reconstructing the geographic ranges of species over key intervals in the past not only offers a means for elucidating macroecological and macroevolutionary dynamics but may help to identify whether small- or large-ranged species are statistically more at risk during extinction events. In the context of the "sixth mass extinction," studies using paleogeographic ranges may therefore help to identify the species most in need of protection (see, e.g., Jablonski and Roy 2003; Lieberman 2004; Payne and Finnegan 2007; Foote et al. 2008, 2016; Lyons et al. 2010; Darroch and Wagner 2015; Saupe et al. 2015).

Despite intensive utilization of paleogeographic ranges for both ecological and evolutionary research, the fidelity with which the fossil record accurately preserves species' ranges is largely unknown. A key question, therefore, is: how accurately are species' geographic range sizes preserved in the geological record? Here, we use simulation experiments to examine (1) the accuracy with which we capture species' paleogeographic range size distributions (i.e., small vs. large ranges) in deep time, (2) the relative performance of four metrics to reconstruct paleogeographic range sizes, and (3) the degree to which we can recover extinction selectivity on range size using fossil occurrences. The first two questions have broad applicability for a wide range of studies focused on macroecological and macroevolutionary patterns in deep time, whereas the last question more specifically tests the extent to which we can potentially use the fossil record of extinction to predict the effects of the ongoing biodiversity crisis.

Methods

To address these questions, we construct a simulations-based framework that reconstructs the paleogeographic range sizes of species using simulated fossil localities placed within the preserved area of sedimentary (and thus potentially fossiliferous) rock from 13 successive geological periods from the Paleozoic. By comparing the sizes of actual and reconstructed ranges for our species, we quantify the accuracy of both absolute and relative range size reconstruction across intervals in Earth's history that have variable spatial distribution and preserved area of sediment. We also simulate variable levels of extinction selectivity with respect to range size, and we quantify the accuracy with which the presence or absence of this selectivity is potentially preserved. All analyses were performed in R version 3.6.2 (R Core Team 2019).

Sedimentary Area and Extant Range Data

We mapped sedimentary rock distributions belonging to 13 geological stages spanning the Carboniferous to the end of the Permian (Kinderhookian–Lopingian; 359.2–251.9 Ma) across the continental United States (see S1 in the supplemental PDF, available online). This study interval is particularly pertinent because repeated sedimentation of offshore marine, nearshore marine, and terrestrial sedimentary rock, known as cyclothems (Heckel 1986), makes the simulations broadly applicable to terrestrial or marine fossil studies. North American geological stages (e.g., Morrowan) were used rather than international standard names to allow for the greatest temporal precision; duration ranged from 1.5×10^6 to 1.9×10^6 years. This temporal resolution was chosen because most paleoecological studies quantify the link between geographic range size and extinction risk (i.e., over mass extinction events) at temporal resolutions of $\sim 10^5$–10^6 years. Sedimentary rock distribution data were derived from United States Geological Survey state-by-state geological maps (https://mrdata.usgs.gov/geology/state/). Sedimentary rock polygons were isolated for a given geological stage in ArcMap and assigned to stage-level time bins based on the formal lithostratigraphic name of their encompassing group, formation, or member using data from the National Geological Map Database (https://ngmdb.usgs.gov/Geolex/search) and extensive review of the literature (see "Stratigraphic References").

We simulated realistic species' paleogeographic range geometries and range size frequencies using polygon distributional data for 341 terrestrial mammals whose ranges extend into the continental United States (taken from the International Union for Conservation of Nature [IUCN] Red List; https://www.iucnredlist.org; fig. 1). These species describe an approximately lognormal distribution of range sizes (S2 in the supplemental PDF) characteristic of many taxonomic groups (Anderson 1977, 1984; Gaston 1996), including many benthic marine invertebrates (Macpherson 2003). We stress that our use of extant mammal ranges does not (for example) assume that ranges of species do not change over geological timescales; extant mammal ranges simply provide us with a realistic framework for the distributions of

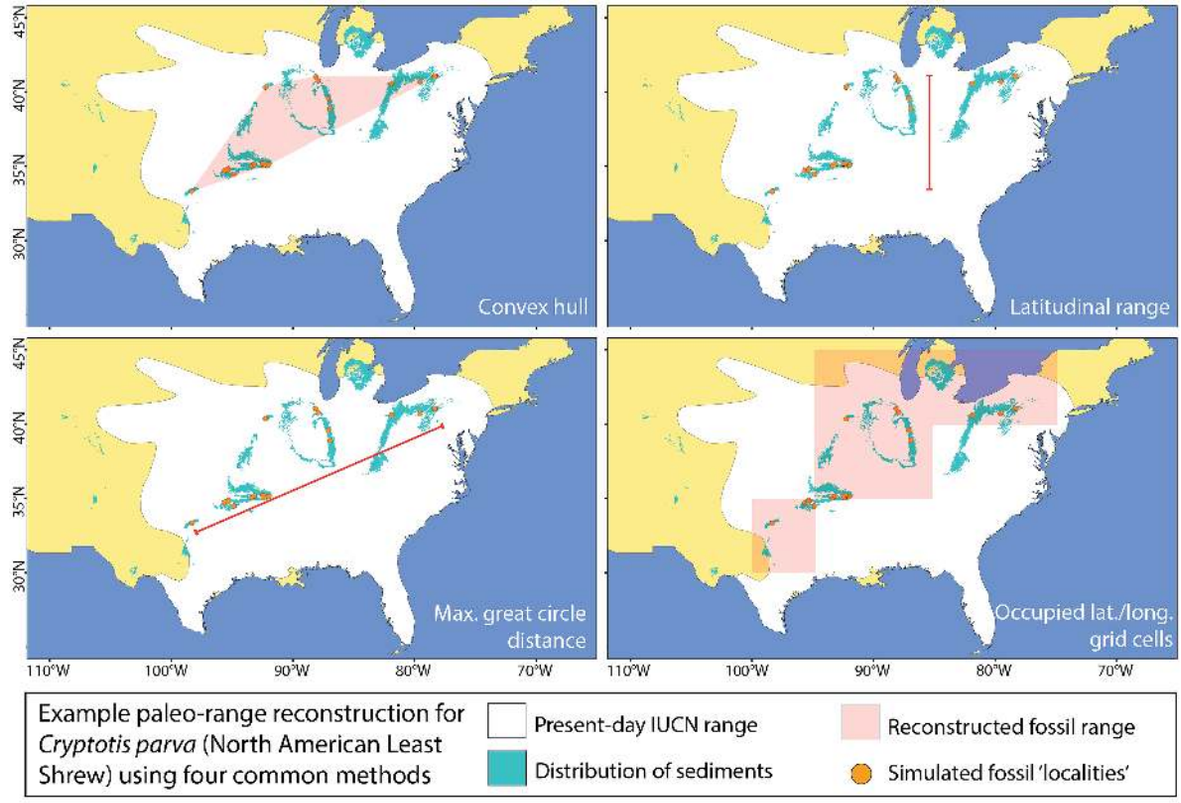

Figure 1: Method for assessing paleo-range size reconstruction using an extant species' range (white; *Cryptotis parva*, the North American least shrew) taken from the International Union for Conservation of Nature (IUCN) Red List and the distribution of fossiliferous sedimentary rock (the Atokan, shown here in green). The overlap between species and fossiliferous sedimentary rock in each geological stage was iteratively seeded with 3–20 randomly placed fossil localities (orange points). From these occurrences, paleo-range size was reconstructed four ways: convex hull, latitudinal range, maximum great circle distance, and number of occupied 5° grid cells.

virtual fossil species, which can represent the time-averaged distributions of species over thousands to millions of years and either marine or terrestrial taxa. Likewise, our use of Paleozoic rock polygons simply provides us with realistic distributions of potentially fossiliferous rocks.

Fossil Site Placement

We used two methods to simulate preservation of fossil localities: by-species site placement and by-sediment site placement. In the by-species method, we placed a given number of sites randomly within each species' polygon. This method for simulating fossil localities allowed us to examine the effect of the number of localities per species on the accuracy of range reconstruction, which is informative for empirical data collection strategy. The procedure, however, clusters sites more densely for species with smaller ranges than for those with larger ranges. Additionally, the approach guarantees that species are sampled when they overlap with sedimentary rock, even if this overlap is minimal (a scenario that would ordinarily be prone to false extinction, i.e., the apparent extinction of a species driven by nonpreservation). An alternative approach, therefore, is to simulate fossil localities randomly within the whole preserved sedimentary rock area. Even if a species' range overlaps with a sedimentary rock layer, it is possible that none of the fossil sites will fall within the area of overlap. This by-sediment site placement method accounts for the low probability of preserving small-ranged species.

In the by-species site placement approach, we drew 3, 5, 7, 10, 15, or 20 "fossil sites" (i.e., occurrences) from each species' original range polygon, to test the sensitivity of range size reconstruction to the number of fossil sites. These numbers reflect the typical range of spatially unique localities characterizing species throughout the Phanerozoic (S3 in the supplemental PDF), and thus they represent realistic scenarios for testing the fidelity of the fossil record. The patchy distribution of sedimentary rocks within each time slice typically resulted in clustered sites (especially in simulations using >10 sites; S4 in the supplemental PDF),

which mirrors empirical patterns in the fossil record shown to be aggregated at all spatial scales (Plotnik 2017). Site placement was iterated for sedimentary rock polygons from each geological stage. Some species' polygons did not overlap with a given sedimentary rock layer, and therefore not all of the 341 virtual species fossilized for every stage. To downweight the importance of any one set of random site placements in later analyses, we iterated placement of sites 100 times.

In the by-sediment site placement approach, we transformed the North American study area to an equal-area grid of 0.5° cells, based on the Albers conic map projection. This step improved computational efficiency. We then simulated fossil species' geographic ranges by iteratively placing 7, 20, 55, 148, 403, or 1,096 sites (an exponential series) across the area of preserved sedimentary rock in each stage. The by-sediment placement method introduced more variance among iterations compared with the by-species method, and so we repeated site placement 200 instead of 100 times. We excluded species that occupied either one or two grid cells from further analysis when using the by-sediment data set, because it was not possible to calculate convex hull area for such species.

Assessment of Paleo-Range Size Reconstructions

We calculated the paleo-range size of each species using four commonly used paleontological methods for range reconstruction (fig. 1; S5 in the supplemental PDF): (1) convex hull area (Stigall and Lieberman 2006; Hendricks et al. 2008; Myers and Lieberman 2010; Raia et al. 2012; Darroch and Wagner 2015; Saupe et al. 2015), (2) maximum great circle distance (Jablonski and Roy 2003; Foote and Miller 2013), (3) latitudinal range (Finnegan et al. 2012; Foote and Miller 2013), and (4) either occupied cells in a 5° latitude/longitude grid for by-species site placement (e.g., Clapham and Payne 2011; Foote 2016) or 0.5° equal-area grid for by-sediment site placement. To mitigate right skew in distributions of range sizes, a natural log transformation was applied to all measurements except counts of grid cells, which were transformed by square root. Hereafter, we define a simulation as the set of replicates run under a given set of parameters listed in table 1 (e.g., by-sediment method, Atokan, 10 sites, latitudinal range).

To quantify the accuracy of reconstructed paleo-range size and extinction selectivity, we calculated the nonparametric (rank-based) correlation between preserved and true range size of all fossil species for each replicate of the 624 simulations (2 site placement methods × 13 stages × 6 site numbers × 4 range metrics). To account for potential ties (e.g., species that occupied the same number of grid cells), we used Kendall's τ correlation coefficient. We summarized τ as the median among replicates of each simulation. Finally, to assess how well each range reconstruction method captured true range size rank order, we used a linear model to predict τ as a function of range reconstruction method (table 2, model 1). Model coefficients were inspected to select the range method associated with the closest correlations between true and fossil range size rank order. To assess the probability that a species would be preserved on the basis of its true range, we also fit a binary logistic regression to predict whether each species was sampled or not in a representative simulation (e.g., Kinderhookian sedimentary rock; 10 sites for by-species placement, and 55 sites for by-sediment placement) as a function of its IUCN geographic range, as measured by the metric selected from model 1 (predicting τ as a function of range reconstruction method).

A second regression was then run to quantify relative influence of preservational predictors on the strength of correlation between fossil and true range size (table 2, model 2). This regression considered only the "best" range reconstruction method selected in the first regression model. We considered up to five parameters as predictor variables in the second regression: area and dispersion of sedimentary rock, number of recovered species, number of sites, and mean fossil range size among species (table 1; S6, S7 in the supplemental PDF). As in the first regression, each variable was summarized for a simulation as the median among replicates. To quantify dispersion of sedimentary rock, we rasterized sedimentary polygons in each stage into 1° latitude/longitude grid cells (S8 in the supplemental PDF); a cell was included if any part of it intersected with sedimentary rock. The centroid of each occupied cell was calculated, and a minimum spanning tree was generated from these centroids (i.e., the shortest distance between all points). Dispersion was recorded as the summed distance of spanning trees (km). Area and dispersion were natural log transformed. We excluded pairs of highly correlated ($\tau > 0.6$) regressor variables, which could cause model misspecification. Although correlation values are bounded by 0 and 1, and thus a linear model could result in unusual end behavior, linearity was justified in this case because observed correlations fall within the midrange only (Long 1997).

Assessment of Extinction Selectivity Estimates

After assessing the fidelity of relative reconstructed range sizes, we examined the accuracy and precision of estimates on extinction selectivity patterns. That is, we tested whether we were able to detect the true signal of extinction selectivity from reconstructed geographic range sizes. We assigned binary extinction status to virtual species based on true IUCN range sizes, such that restricted species faced a higher risk of extinction than widespread species. We then predicted survival outcome as a function of reconstructed fossil

Table 1: Parameters of simulations

Parameter	Levels/values	Application
Site placement	By-species or by-sediment method	Range fidelity
Range metric	Convex hull area, maximum great circle distance, latitudinal range, occupied grid cell count	Range fidelity
Sites	3, 5, 7, 10, 15, 20 for by-species method; 7, 20, 55, 148, 403, 1,096 for by-sediment method	Range fidelity and extinction selectivity
Sedimentary rock coverage	Area and dispersion of 13 stages	Range fidelity and extinction selectivity
Extinction intensity	25%, 50%, 75%	Extinction selectivity
Survivorship model	Null (random) or selective against small-ranged species based on the inverse logit of geographic range size (see S9 in the supplemental PDF)	Extinction selectivity
Species n	Forced removal of no species, one-third of species, or two-thirds of species	Extinction selectivity
False extinction	False (not allowed) or true (apparent extinction of species due to geographic shifts in the sedimentary rock record)	Extinction selectivity

Note: Shown are parameters that were experimentally manipulated in simulations to assess paleogeographic range fidelity and/or extinction selectivity. Fossil sampling sites were placed such that a given number were either within each species' range overlap with sedimentary rock (by-species method) or across the entire sedimentary rock area at random with respect to species (by-sediment method). The 13 sedimentary rock areas were derived from 13 geological stages spanning the Carboniferous to the end of the Permian (Kinderhookian–Lopingian). To simulate false extinction, we checked for species that had been assigned as extinction survivors but were not sampled in the time bin immediately following the focal stage; the status of these species was changed to "victim."

paleo-range sizes. We measured fossil ranges with the single range reconstruction metric determined to be most accurate based on the first metaregression of range size reconstruction fidelity ("Assessment of Paleo-Range Size Reconstructions" above). We extracted the model coefficient β, which corresponds to the estimated increase in log-likelihood extinction risk per unit increase in geographic range size. We compared the β from each simulation (median among replicates) to the true value (which we set a priori as equal to 1) to assess accuracy of extinction selectivity estimates, and we calculated the standard deviation of β to assess precision.

Probability of survival was calculated as the inverse logit of natural-log-transformed IUCN range polygon area. Thus, smaller ranges conferred greater risk of extinction, but the magnitude of this effect lessened at extremely large or small values (S9 in the supplemental PDF). This assumed relationship between extinction risk and range size is intuitive

Table 2: Linear regression models

Model	Application	Extinction model	False extinctions	Model formula
1	Range fidelity	...	...	Median(τ) ~ range metric
2	Range fidelity	...	...	Median(τ) ~ dispersion + n species sampled + sites
3	Extinction selectivity	Null	Ignored	Median(β) ~ dispersion + n species sampled + sites + extinction threshold
4	Extinction selectivity	Null	Ignored	SD(β) ~ dispersion + n species sampled + sites + extinction threshold
5	Extinction selectivity	Null	Allowed	Median(β) ~ dispersion + n species sampled + sites + extinction threshold + n false extinctions
6	Extinction selectivity	Null	Allowed	SD(β) ~ dispersion + n species sampled + sites + extinction threshold + n false extinctions
7	Extinction selectivity	Selective	Ignored	Same as model 3
8	Extinction selectivity	Selective	Ignored	Same as model 4
9	Extinction selectivity	Selective	Allowed	Same as model 5
10	Extinction selectivity	Selective	Allowed	Same as model 6

Note: Shown are linear regression models, numbered in order of use. For range fidelity models, the response variable was Kendall's τ correlation between true and preserved range size. For extinction selectivity models, the response variable was the per-species increase in extinction risk per unit geographic range size (the β coefficient extracted from previous binary logistic regressions) or the standard deviation (SD) thereof. The β coefficient and its SD are interpreted as the accuracy and precision, respectively, of reconstructed selectivity. Extinction was either selective against narrowly distributed species (S9 in the supplemental PDF) or random with respect to range size (i.e., null). We repeated simulations with and without the inclusion of false extinctions (described in table 1).

and carries the consequence that a logistic regression of survival probability as a function of IUCN range size would fit perfectly, with R^2 and β coefficient both equal to 1. That is to say, this probabilistic manner of assigning extinction status means that we know the true underlying relationship between range size and extinction risk, and so we can quantify the accuracy of the relationship estimated from the fossil species in our simulations by comparing the simulated relationship, β, to the known relationship (1.0). Furthermore, we evaluated the probability of recovering a selectivity signal when there were no underlying selectivity patterns; that is, we evaluated how frequently type 1 errors could occur in studies of extinction selectivity. We interrogated this question by selecting "victims" and "survivors" at random rather than on the basis of geographic range size and comparing the simulated extinction selectivity, β, to the known value of 0.

Assignment of extinction outcomes was repeated for each iteration of random site placement for every simulation. We conducted each set of replications under three intensities of extinction: 25%, 50%, and 75% species loss. These thresholds were implemented by shifting the distribution of true range size left by a distance proportional to the desired quantile of extinction. For instance, median range size was subtracted from the range size distribution before calculating survival probability in order to achieve an expected extinction rate of 50%.

We note that in this extinction assignment framework, we a priori assume that range size is a predictor of extinction risk and test whether this signal can be recovered in simulations. Therefore, our study does not test explicitly whether range size is a strong predictor of empirical extinction risk, but rather it tests the degree to which the signal can be recovered from realistic fossil locality data.

In addition to extinction intensity, we manipulated two other variables in extinction selectivity simulations. First, we experimentally removed either two-thirds, one-third, or no species a priori. This step allowed metaregression analysis to distinguish the independent effect of sample size (number of species) from sedimentary rock coverage; otherwise, more species tended to be sampled in stages with larger preserved rock areas. Second, we considered the possibility of "false extinctions"—that is, species that survived a given interval but were sampled only in the first time bin and not the subsequent one. We calculated preserved ranges of all species in a given time bin, assigned binary extinction status, and checked which of those species were sampled in the subsequent time bin. For any species sampled in the first bin and assigned as survivors but not sampled in the latter time bin, the status was changed to victim (a purposely incorrect designation). For this purpose, the earliest time bin (Kinderhookian) was simulated as if it followed from the latest time bin (Lopingian).

We fit an initial binary logistic regression model to predict extinction outcome as a function of preserved range size for every replication of a simulation. We extracted the β coefficient, representing the estimated increase in survival probability per unit range size. The β coefficient estimated for a model with perfect knowledge of range size and all available species would be 1 because that probability of survival was based solely on true range size (as detailed above); thus, β can be interpreted as proportional accuracy in estimated selectivity strength (hereafter referred to as "selectivity accuracy"). The accuracy and precision estimates were summarized for each simulation as the median and standard deviation of τ values from all iterations of site placement and extinction outcome assignment.

We quantified the relative influence of simulation parameters on selectivity accuracy in regressions (table 2). Since binary logistic regressions had been run to generate β values, subsequent models built to predict β values (models 3–10) were technically metaregressions. The possible predictor variables explored during model selection were the same as those used in the second metaregression examining range size fidelity (dispersion of sedimentary rock, number of sampled species, number of sites, and mean fossil range size among species), with the addition of extinction threshold and number of false extinctions (tables 1, 2). In total, we fit eight metaregressions, one for each combination of selective or null (random) extinction assignments, inclusion or exclusion of false extinctions, and accuracy or precision as the response variable (table 2). Each sample in the metaframework consisted of the median value among replicates of site placement for a given simulation, to prevent pseudoreplication from iterating each simulation 100 or 200 times. Thus, each metaregression was trained on 702 observations: 6 site numbers × 13 stages × 3 extinction intensities × 3 species removal thresholds. All data and files underlying analyses have been deposited in GitHub (https://github.com/GwenAntell/ExtSelectivity2020; Darroch et al. 2020).

Results

Accuracy of Paleo-Range Size Reconstruction, By-Species Site Placement

Of 341 species, 85–237 preserved within the 13 sedimentary rock polygons (S6 in the supplemental PDF). The median fossil range size of each range reconstruction method (median among replicates for each species, then among species and simulation experiments) was 2.35×10^4 km^2 convex hull area, 5.07×10^2 km maximum great circle distance, 3.00 grid cells (initial 5° resolution), and 2.99° latitudinal range. True (IUCN) median geographic range size among all species, regardless of whether they fossilized, was

3.76×10^5 km^2 convex hull area, 1.46×10^3 km maximum great circle distance, 1.40 × 10 grid cells, and 10.4° latitudinal range. Correlation coefficients (Kendall's τ) between the rank order of preserved fossil and true IUCN geographic range sizes varied from 0.22 to 0.67 (mean $= 0.45 \pm 0.10$; fig. 2*A*, 2*C*).

Range method alone explained little variance in τ ($R^2 = 0.09$), as estimated in model 1, which tested how well each range reconstruction method captured true range size rank order (table 3). The metric associated with the largest τ values (i.e., highest accuracy) was convex hull area, followed in order by grid cell count, maximum great circle distance, and latitudinal range (table 3). The estimated amount of truncation in convex hull area due to fossilization was 0.67 on a natural log scale (S10 in the supplemental PDF)—an average reduction by two orders of magnitude (0.02 of original size) on an untransformed scale. Among our candidate variables to predict correlation strength, sedimentary rock area correlated strongly with sediment dispersion ($\tau = 0.64$) and number of species preserved in a stage ($\tau = 0.62$; S11 in the supplemental PDF). Therefore, according to our a priori criterion to avoid excessive correlation in regressor variables, sedimentary rock area was omitted as a predictor in the regression that quantified relative influence of preservational predictors on the strength of correlation between fossil and true range size (table 2, model 2). Similarly, the number of sites correlated tightly ($\tau = 0.69$; S11 in the supplemental PDF) with preserved convex hull area, and so the latter was omitted as a predictor. All remaining predictors (natural log number of sites, natural log sedimentary rock dispersion, and number of species preserved) explained most of the variance in τ values among simulations ($R^2 = 0.84$). In particular, the correlation between rank-order preserved range size and true geographic range size increased as a function of each of these predictor variables (table 4).

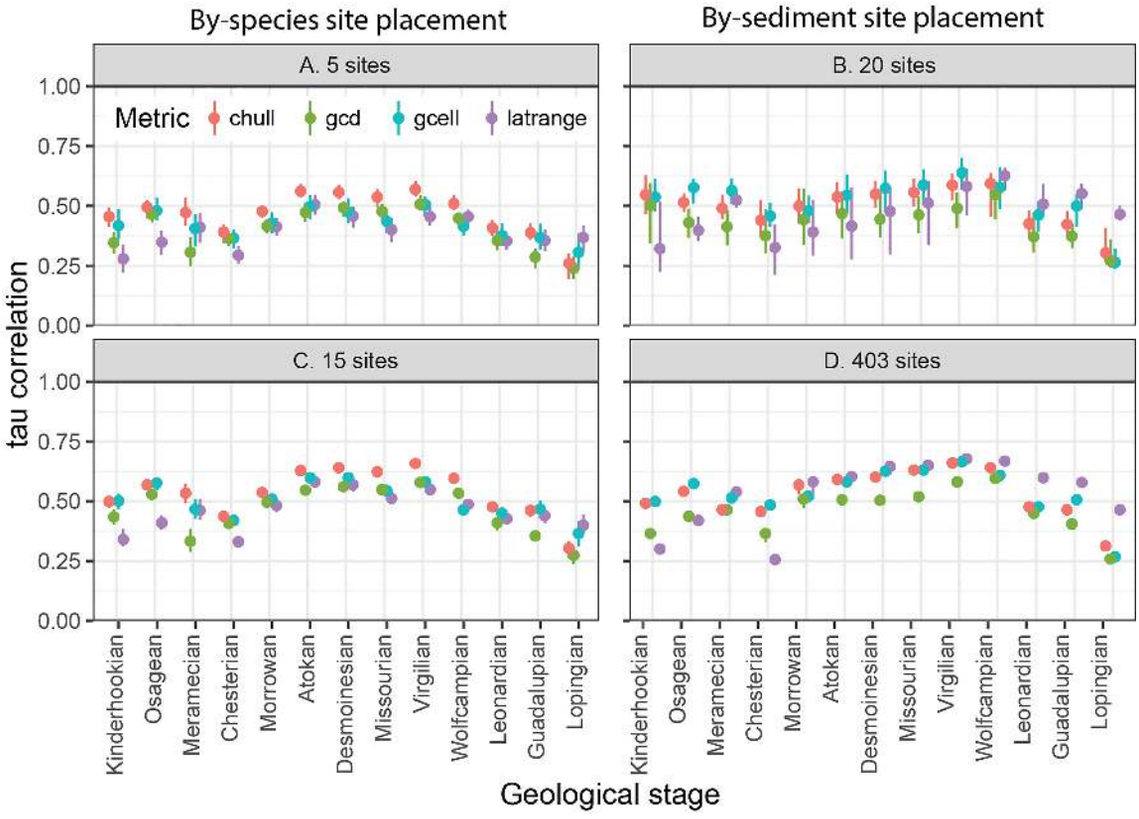

Figure 2: Rank-based correlations (Kendall's τ) between actual and simulated geographic paleo-range sizes, illustrating general high agreement throughout the studied interval. By-species site placement is shown in *A* and *C*, and by-sediment site placement is shown in *B* and *D*. For clarity, only two of six values of site numbers are displayed. Error bars show 90% quantiles of values among iterations. Error bars are larger when the number of sites is lower (*A* and *B* vs. *C* and *D*), and τ values are higher when paleogeographic range size is measured as a two-dimensional metric (convex hull area [chull] and grid cell count [gcell]) rather than as a one-dimensional metric (latitudinal range [latrange] and maximum great circle distance [gcd]).

Table 3: Regression coefficients for model 1

Method, metric	Estimate	SE	*t*	*P*
By-species site placement:				
Intercept	.493	.010	47.035	.000
gcd	−.067	.015	−4.545	.000
gcell	−.038	.015	−2.594	.010
latrange	−.073	.015	−4.892	.000
By-sediment site placement:				
Intercept	.515	.011	47.439	.000
gcd	−.072	.015	−4.673	.000
gcell	.013	.015	.822	.412
latrange	−.010	.015	−.684	.495

Note: Regression coefficients are reported from model 1 (table 2), the prediction of range fidelity as a function of paleogeographic range metrics. Range fidelity was parameterized as Kendall's τ correlation between preserved and true paleogeographic range sizes, summarized as the median among iterations. The R^2 value for the model corresponding to by-species site placement data was 0.089, and that for by-sediment site placement was 0.104. Range metric was one of convex hull area (the baseline against which the others coefficients are relative), maximum great circle distance (gcd), grid cell count (gcell), or latitudinal range (latrange).

Accuracy of Paleo-Range Size Reconstruction, By-Sediment Site Placement

Between 87 and 226 species were preserved and sampled within the 13 sedimentary rock polygons. The median fossil range size of each range reconstruction method (median among replicates for each species, then among species and simulation experiments) was 1.26×10^5 km^2 convex hull area, 7.81×10^2 km maximum great circle distance, 7.00 grid cells, and 4.55° latitudinal range. The median IUCN range sizes, when rasterized into equal-area grid cells, were 1.27×10^6 km^2 convex hull area, 2.06×10^3 km maximum great circle distance, 334 grid cells (initial 0.5° resolution), and 13.7° latitudinal range. Correlation coefficients between the rank order of preserved fossil and true IUCN geographic range sizes varied from 0.26 to 0.68 (mean $= 0.50 \pm 0.10$; fig. 2*B*, 2*D*).

Range reconstruction method alone explained little variance in τ ($R^2 = 0.10$), as estimated in model 1 (table 3). Convex hull area, grid cell count, and latitudinal range were associated with the largest τ values (i.e., highest accuracy), whereas maximum great circle distance performed substantially worse (table 3; fig. 2*B*, 2*D*). We based subsequent models on convex hull area measurements for consistency with the by-species site placement analyses, although this metric performed equivalently well relative to two others (grid cell count and latitudinal range). The estimated amount of truncation in convex hull area due to fossilization was 0.82 on a natural log scale (S12 in the supplemental PDF)—an average reduction by one order of magnitude (0.09 of original size) on an untransformed scale. For every 1-unit increase in convex hull area (natural log scale), species were 6.0 times more likely to be sampled as fossils (95% confidence interval = 3.9–9.6). The area of sedimentary rock correlated strongly with sediment dispersion and with the number of species (S13 in the supplemental PDF), so area was excluded as a predictor in later by-sediment analysis (as in by-species analysis). Preserved convex hull area increased in step with the number of sites used for reconstruction ($\tau = 0.68$; S13 in the supplemental PDF), so mean convex hull area was also excluded as a predictor. All of the remaining predictors (natural log number of sites, natural log sedimentary rock dispersion, and number of species preserved) explained most of the variance in τ values among simulations ($R^2 = 0.79$). In particular, the correlation between rank order for preserved and true geographic range size increased as a function of each of these predictor variables (table 4).

Accuracy and Precision of Extinction Selectivity Reconstruction, By-Species Site Placement

Regression of logit survival probability on fossil range size recovered a positive relationship (i.e., widespread species were predicted to survive more often than restricted species). The mean value of β (the increase in log-likelihood extinction risk per unit increase in geographic range size) in simulations excluding false extinctions was 0.270, with a 90% quantile of [0.170, 0.420] (S14A in the supplemental PDF). That is to say, nearly every simulation correctly identified the direction of selectivity but consistently underestimated the magnitude of the true value (unity). Fossil estimates of extinction intensity were also lower than the

Table 4: Regression coefficients for model 2

Method, metric	Estimate	SE	*t*	*P*
By-species site placement:				
Intercept	−.808	.081	−10.008	.000
gcd	.076	.008	9.994	.000
gcell	.123	.010	11.714	.000
latrange	.001	.000	3.867	.000
By-sediment site placement				
Intercept	−.462	.075	−6.130	.000
gcd	.009	.003	3.422	.001
gcell	.092	.010	9.306	.000
latrange	.001	.000	6.569	.000

Note: Regression coefficients are reported from model 2 (table 2), the prediction of range fidelity as a function of the number of sites (log transformed), minimum spanning tree length of sedimentary rock area (dispersion, log transformed), and number of species preserved (species *n*). The R^2 value for the model corresponding to by-species site placement data was 0.835, and that for by-sediment site placement was 0.789. Paleogeographic range size was measured as convex hull area.

true values (S16, S17 in the supplemental PDF) because narrowly distributed species that became extinct were never observed in the first place.

Summarizing among metaregression results, parameters were influenced by several key factors (S14, S15 in the supplemental PDF). For instance, more fossil sites led to greater accuracy of selectivity estimates (larger β values) but had little detectable influence on the precision of estimated selectivity. In fact, precision decreased (larger standard deviation of β) when more sites were added under null (random) selectivity. The effect of sedimentary rock dispersion also varied depending on whether extinction was random or selective. In selective simulations, accuracy but not precision increased with greater preserved rock coverage. In contrast, under random extinction, sedimentary rock dispersion had a negligible or negative effect. The effect of extinction magnitude varied widely among simulations and was unclear overall (figs. 3, 4; S14, S15 in the supplemental PDF). Larger sample size (fewer species removed a priori, independent of the number of extinctions) led to both more accurate (S14 in the supplemental PDF) and more precise (S15 in the supplemental PDF) estimates.

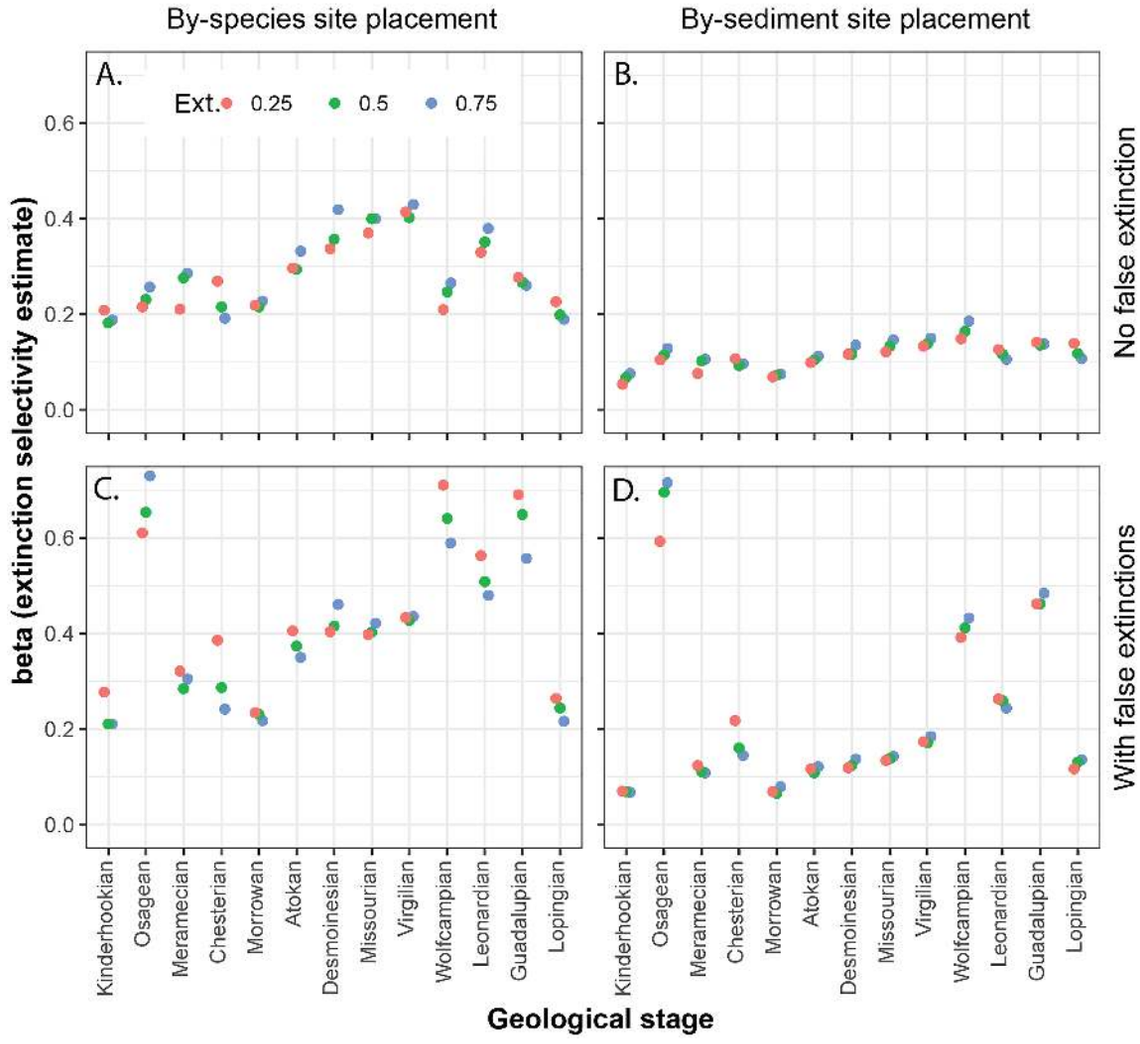

Figure 3: Accuracy of selectivity reconstruction (i.e., mean of β, the per-species increase in extinction risk per unit range size), illustrating correct detection of the direction of selectivity under all extinction intensities. Extinction was selective against narrowly distributed range sizes (see fig. 4 for random extinction). In *A* and *B*, no false extinctions were simulated; in *C* and *D*, false extinctions were included. Data are from by-species site placement in *A* and *C* and from by-sediment site placement in *B* and *D*. In the case where false extinction was not simulated, values in different stages are entirely independent; that is, chronological order is irrelevant to β values. Color indicates the true extinction rate (25%, 50%, or 75%).

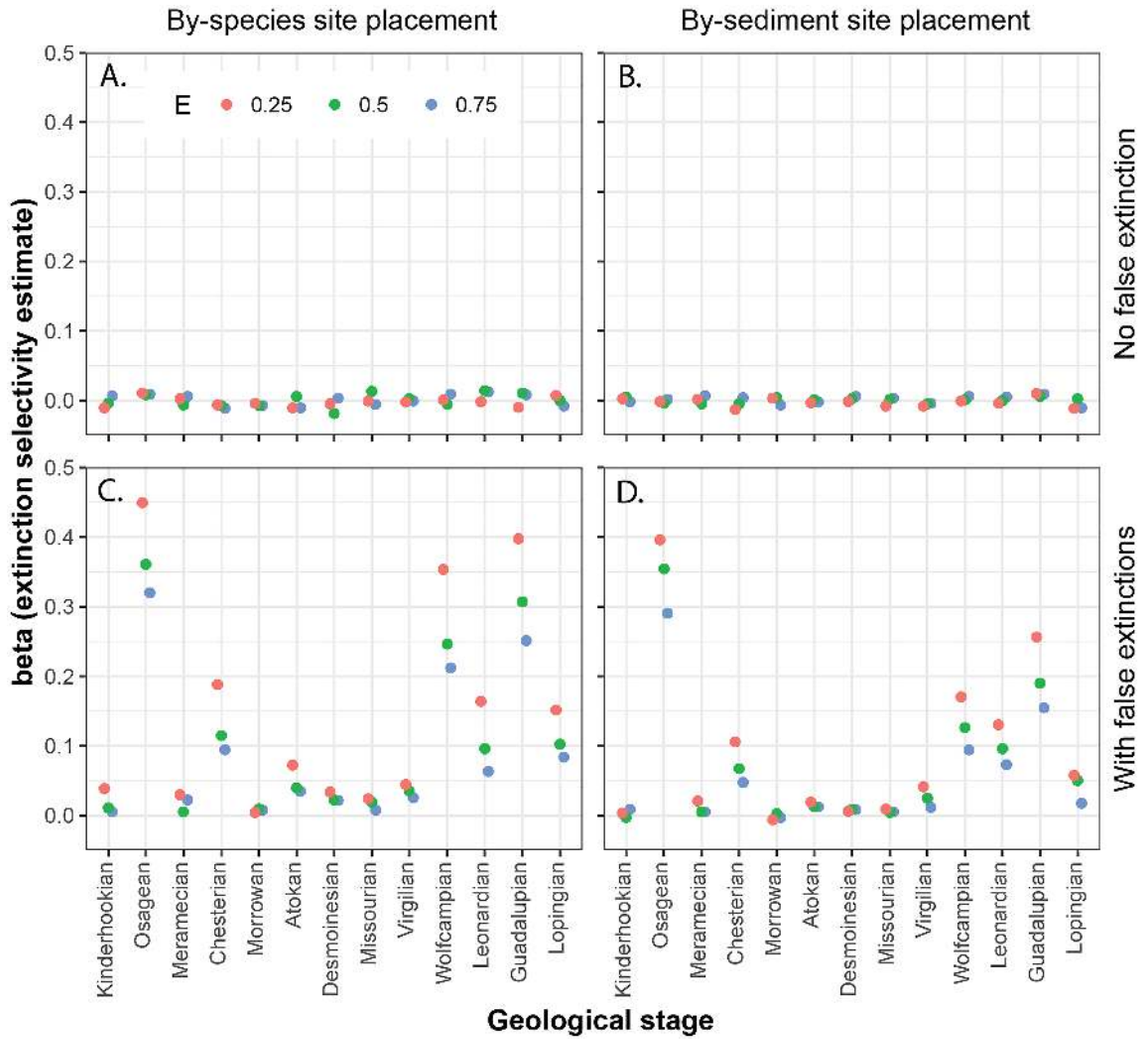

Figure 4: Accuracy of selectivity reconstruction (i.e., mean of β, the per-species increase in extinction risk per unit paleo-range size) when extinction was random with respect to species' range sizes (see fig. 3 for selective extinction). Any value more than zero is an overestimate that could be interpreted as a false-positive signal of extinction selectivity. In *A* and *B*, no false extinctions were simulated; in *C* and *D*, false extinctions were included. Introducing false extinctions thus resulted in a marked increase in false-positive extinction selectivity signals. Data are from by-species site placement in *A* and *C* and from by-sediment site placement in *B* and *D*. Color indicates the true extinction rate (25%, 50%, or 75%).

The number of false extinctions incurred for a simulation strongly predicted β coefficients. The more false extinction events, the larger the selectivity estimate (figs. 3, 4; S14, S15 in the supplemental PDF). β coefficients in null simulations that permitted false extinctions were greatly inflated (mean = 0.108; 90% quantile = $[0.001, 0.370]$) compared with those from simulations that considered only a static time interval (mean = more than -0.001; 90% quantile = $[-0.020, 0.020]$; S14 in the supplemental PDF). The same trend occurred in selective simulations: selectivity estimates were higher when simulations included false extinctions (mean = 0.394; 90% quantile = $[0.198, 0.705]$) than when they excluded them (mean = 0.270; 90% quantile = $[0.170, 0.420]$; S14 in the supplemental PDF).

Accuracy and Precision of Extinction Selectivity Reconstruction, By-Sediment Site Placement

Regressions identified the direction but underestimated the magnitude of extinction selectivity, congruent with the results from fossil distributions generated with by-species site placement. Many of the estimated effects of predictor variables were similar as well. For instance, placing more fossil

sites generally led to greater accuracy but had little detectable influence on the precision of estimated selectivity (S14, S15 in the supplemental PDF). Larger signals of selectivity were also detected when sedimentary rock coverage was larger.

The effects of extinction magnitude and number of species sampled were complex: although higher extinction rates and larger sample sizes corresponded to more accurate and precise estimates in selective simulations, there was little correspondence under random extinction. One exception is that when false extinctions were excluded and extinction was random, β values were falsely inflated at high extinction values. When false extinctions were included in random or selective simulations, β values were inflated even further (figs. 3, 4). For null selectivity, β coefficients from simulations that permitted false extinctions (mean $= 0.102$; 90% quantile $= [-0.003, 0.488]$) were larger than those from simulations that considered only a static time interval (mean = more than -0.001; 90% quantile $= [-0.016, 0.016]$; S14 in the supplemental PDF). The same trend occurred in selective simulations: selectivity estimates were higher when simulations included false extinctions (mean $= 0.303$; 90% quantile $= [0.070, 0.887]$) than excluded them (mean $= 0.169$; 90% quantile $= [0.061, 0.402]$; S14 in the supplemental PDF). Furthermore, the R^2 values of models based on simulations with false extinctions were higher than those without (S14 in the supplemental PDF), attesting to the explanatory value of false extinction count.

Discussion

Our results show that relative paleogeographic range size is preserved with surprising accuracy in all four methods used in this study (fig. 2). For example, even the least accurate range size reconstruction from simulations using the by-species site placement method ($\tau = 0.32$) recovered true rank order of range size surprisingly well—this simulation re-created range size order despite the paucity of sedimentary rock (~7,000 km^2, based on Lopingian formations), low recovery of species (123 of 341 species fossilized), and small number of fossil sites (three per species, the minimum required to calculate a convex hull). This in turn suggests that paleogeographic ranges reconstructed from fossil data can be used to test a wide range of macroevolutionary and macroecological models in deep time, such as whether large range sizes were associated with more (or less) rapid rates of speciation (e.g., Jablonski and Roy 2003), lower rates of extinction (e.g., Harnik et al. 2012), or greater habitat breadth (e.g., Nurnberg and Aberhan 2013).

Of the four range reconstruction methods analyzed, two-dimensional metrics (convex hull area and grid cell count) generated more concordant rank orders between fossil and modern geographic ranges than did one-dimensional metrics (latitudinal range and maximum great circle distance; fig. 2). We note, however, that the four methods tested here provide slightly different measures of geographic range. For example, latitudinal range is commonly taken to provide a measure of thermal tolerance, whereas maximum great circle distance, convex hull, and number of occupied grid cells provide measures of absolute range size and/or breadth of habitat preference (Hendricks et al. 2008). Choice of method will therefore reflect the nature of the question posed. We also acknowledge that while two-dimensional metrics may perform best for the broad swathe of Paleozoic time considered here, specific intervals (with specific configurations of marine sediments) may behave differently. For example, in more recent parts of the Cenozoic, marine sediment is concentrated along coastlines (i.e., north-south). In these scenarios, a one-dimensional metric like latitudinal range might perform better than in the simulated sediment configuration.

Our analyses of extinction selectivity on range size detected the direction of selectivity under all extinction intensities (25%, 50%, and 75%; fig. 3). Moreover, our simulations illustrate that sedimentary rock area affects our ability to reconstruct signals of extinction selectivity in that the accuracy with which we detect extinction selectivity on range size increases with the dispersion of preserved sedimentary rock. This result suggests that dramatic eustatic changes in sea level associated with many extinctions (such as the late Ordovician and end Cretaceous) may significantly affect our ability to reconstruct range size–extinction risk signals over these events, especially if these changes led to a dramatic reduction in sedimentary rock preservation. Our simulation framework, however, is likely conservative with regard to the pattern of increased accuracy with size of preserved geographic ranges. Given the relative paucity of geographic barriers in shallow marine environments and the ease with which many marine species can disperse, geographic ranges of marine species are typically larger than terrestrial species (Gaston 1996; Tomašových et al. 2016). Since range size is an important determinant of whether species are recorded in the rock record (and larger range sizes lead to increased accuracy in reconstructing extinction patterns), empirical analysis on marine species may be even more accurate than our simulations would suggest.

False extinctions (i.e., the apparent extinction of a species as a result of geographic shifts in the sedimentary rock record) inflated estimates of extinction selectivity and induced false signals of selectivity in nonselective simulations (fig. 4). Indeed, selectivity estimates in some null simulations were as high, or higher, than those from selective simulations. Since the probability that a geographic range will overlap sedimentary rock decreases with range size, it is likely that most species that experienced false extinction were

narrowly distributed. Therefore, these species introduced the same pattern that would occur if narrowly distributed species truly—not falsely—became extinct. Imprecision in the temporal aspect of extinctions (timing of the event) could therefore affect selectivity analysis far more than imprecision in the geographic component (characterization of species' range size). There are several ways to reduce the incidence of false extinction and thence inflated selectivity estimates. For instance, during field exploration it is important to work updip or downdip in a stratigraphic section to search for a species in equivalent environments before and after an extinction event (Holland and Patzkowsky 2015; Holland 2020). At the analysis stage, "range-through" methods and control of edge effects could further reduce the frequency of false extinction.

We acknowledge that our analytical framework has several potential limitations that may impact the interpretation of results. First, we note that we use biological species for our ranges, while a majority of empirical paleontology studies operate at the genus level. Lumping species into genera would typically be expected to result in larger ranges (and thus lower incidences of false extinction). However, other authors note that (1) fossil genera are frequently nonequivalent collections of species will little to no biological reality of their own and (2) attributes considered important for understanding macroevolution (including geographic ranges) are frequently variable among species within genera (Hendricks et al. 2014). Therefore, while using genera would likely lead to higher fidelity in preservation of range sizes (and range selectivity signals) in our experiments, the applicability of these results to studying macroecological and macroevolutionary patterns may be dampened. Second, although our method for simulating fossil sites typically produced highly clustered patterns of occurrences similar to those exhibited by the fossil record (Plotnik 2017; S4 in the supplemental PDF), we assumed individual species preserve equally well across their spatial distribution, which is unlikely to be the case (Noto 2010). Third, our framework also assumed equal preservation potential across all species, whereas a number of factors, including body size, population size, and mortality rate, can affect the likelihood of fossilization (Behrensmeyer 1978; Fraser 2017; Plotnik 2017; Darroch and Saupe 2018). Although varying the preservation potential of individual species across their ranges is beyond the scope of this particular study, future iterations of this analytical framework will examine if—and how—such factors affect the accuracy with which we can reconstruct extinction selectivity patterns in deep time. We also assume that similar habitats (i.e., sedimentary facies and subenvironments) are sampled in adjacent time bins and acknowledge that we are limited to Carboniferous sedimentary rock configurations. This latter assumption maybe conservative, however, as preserved ranges may have higher fidelity in more recent time bins, when there tends to be larger areas of preserved sedimentary rock.

We emphasize that this study provides the first concerted attempt to calibrate the quality of the spatial fossil record in the distant geological past and that our simulations thus far indicate that the fossil record comprises a powerful spatial and biogeographic data set, with respect to preserving both the rank order of geographic range sizes and extinction selectivity patterns. Although the rank order of geographic ranges has high preservation potential, absolute geographic range size does not—range sizes were truncated significantly (approximately by one order of magnitude) in simulations, which has implications for how fossil range data are used to inform conservation decisions today. For example, the IUCN currently defines specific range size thresholds (together with subsidiary criteria typically not accessible in fossil data) for determining extinction risk status of species. Since our simulations suggest that absolute range size has poor preservation potential, identifying a specific threshold of geographic range size under which fossil species have tended to become extinct over past biotic crises is likely untenable. Our simulations do suggest, however, that we can accurately determine whether range size was a determinant of extinction risk during intervals that varied in extinction intensity, which provides information relevant to the current biodiversity crisis and ongoing conservation efforts (Finnegan et al. 2015) and will help to identify at-risk species in a range of future global change scenarios.

In summary, our simulations suggest that relative paleogeographic range size can be faithfully preserved in the rock record, even in intervals possessing scarce sedimentary rock areas. Furthermore, simulations provide confidence that we can determine the magnitude and direction of the relationship between extinction risk and geographic range size in deep time. However, our simulations also suggest that type 1 errors (i.e., false positive range size–extinction risk signals) may be prevalent, in particular when the distribution of environments represented by sedimentary rocks change dramatically between time slices (leading to false extinction). To be clear, our simulations do not have any bearing on whether paleo-range size is an important predictor of extinction risk over intervals of mass extinction—previous studies have argued both that they are (Payne and Finnegan 2007; Jablonski 2008) and that they are not (Jablonski 1986, 2003). Rather, our study interrogates whether selectivity of extinction on range size can be estimated accurately from fossil locality data in the paleontological record using a simulation approach. Our results demonstrate that during episodes of moderate to intense extinction (25%–75% species loss), we can determine whether paleogeographic range size is correlated with extinction risk. Furthermore, our results reinforce the inference that the

fossil record represents an invaluable biogeographic data set and natural laboratory for reconstructing macroecological and macroevolutionary patterns over critical intervals in Earth's history.

Acknowledgments

This study was inspired by discussions with Doug Erwin, Pete Wagner, Kate Lyons, Joshua Miller, and Pincelli Hull (among many others). M.M.C. and E.E.S. acknowledge funding from National Science Foundation grants DEB-1256993 and EF-1206757NSF to Bruce Liebermann. E.E.S. also acknowledges generous support from the Leverhulme Foundation (grant DGR01020). For the analyses contained within the supplemental PDF, we thank all contributors to the Paleobiology Database. The authors declare no competing interests.

Statement of Authorship

S.A.F.D., M.M.C., G.S.A., and E.E.S. designed the study. M.M.C. and A.S. compiled .shp files for the geological stages used in simulations. S.A.F.D, G.S.A., and E.E.S. analyzed the data. G.S.A. wrote the final analysis code. S.A.F.D., E.E.S., and M.M.C. managed and supervised the project. All authors wrote the manuscript.

Data and Code Availability

All raw data, output files, and R scripts necessarily to replicate the study are maintained on GitHub (https://github.com/GwenAntell/ExtSelectivity2020) and are archived at Zenodo (https://zenodo.org/record/3765445#.Xx6SnOfTWUk).

Literature Cited

Aberhan, M., and T. K. Baumiller. 2003. Selective extinction among Early Jurassic bivalves: a consequence of anoxia. Geology 31:1077–1080.

Anderson, S. 1977. Geographic ranges of North American terrestrial mammals. American Museum Novitates 2629:1–15.

———. 1984. Geographic ranges of North American birds. American Museum Novitates 2785:1–15.

Barnosky, A. D., N. Matzke, S. Tomiya, G. O. U. Wogan, B. Swartz, T. B. Quental, C. Marshall, et al. 2011. Has the Earth's sixth mass extinction already arrived? Nature 471:51–57.

Behrensmeyer, A. K. 1978. Taphonomic and ecologic information from bone weathering. Paleobiology 4:150–162.

Botts, E. A., B. F. N. Erasmus, and G. Alexander. 2013. Small range size and narrow niche breadth predict range contractions in South African frogs. Global Ecology and Biogeography 22:567–576.

Brown, J. H., G. C. Stevens, and D. M. Kaufman. 1996. The geographic range: size, shape, boundaries, and internal structure. Annual Review of Ecology, Evolution, and Systematics 27:597–623.

Button, D. J., G. T. Lloyd, M. D. Excurra, and R. J. Butler. 2017. Mass extinctions drove increased global faunal cosmopolitanism on the supercontinent Pangaea. Nature Communications 8:733. https://doi.org/10.1038/s41467-017-00827-7.

Cardillo, M., J. S. Huxtable, and L. Bromham. 2003. Geographic range size, life history, and rates of diversification in Australian mammals. Journal of Evolutionary Biology 16:282–288.

Clapham, M. E., and J. L. Payne. 2011. Acidification, anoxia, and extinction: a multiple logistic regression analysis of extinction selectivity during the Middle and Late Permian. Geology 39:1059–1062.

Darroch, S. A. F., M. M. Casey, G. S. Antell, A. Sweeney, and E. E. Saupe. 2020. Data from: High preservation potential of paleogeographic range size distributions in deep time. American Naturalist, GitHub, https://github.com/GwenAntell/ExtSelectivity2020.

Darroch, S. A. F., and E. E. Saupe. 2018. Reconstructing geographic range size dynamics from fossil data. Paleobiology 44:25–39.

Darroch, S. A. F., and P. J. Wagner. 2015. Response of beta diversity to pulses of Ordovician–Silurian mass extinction. Ecology 96:532–549.

Darroch, S. A. F., A. E. Webb, N. Longrich, and J. Belmaker. 2014. Paleocene–Eocene evolution of beta diversity among ungulate mammals in North America. Global Ecology and Biogeography 23:757–768.

Finnegan, S., S. C. Anderson, P. G. Harnik, C. Simpson, D. P. Tittensor, J. E. Byrnes, Z. V. Finkel, et al. 2015. Paleontological baselines for evaluating extinction risk in the modern oceans. Science 348:567–570.

Finnegan, S., N. Heim, S. Peters, and W. W. Fischer. 2012. Climate change and the selective signature of the Late Ordovician mass extinction. Proceedings of the National Academy of Sciences of the USA 109:6829–6834.

Foote, M. 2016. On the measurement of occupancy in ecology and paleontology. Paleobiology 42:707–729.

Foote, M., J. S. Crampton, A. G. Beu, and R. A. Cooper. 2008. On the bidirectional relationship between geographic range and taxonomic duration. Paleobiology 34:421–433.

Foote, M., and A. I. Miller. 2013. Determinants of early survival in marine animal genera. Paleobiology 39:171–192.

Foote, M., K. A. Ritterbush, and A. I. Miller. 2016. Geographic ranges of genera and their constituent species: evolutionary dynamics, and extinction resistance. Paleobiology 42:269–288.

Fraser, D. 2017. Can latitudinal richness gradients be measured in the terrestrial fossil record? Paleobiology 43:479–494.

Gaston, K. J. 1996. Species-range-size distributions: patterns, mechanisms and implications. Trends in Ecology and Evolution 11:197–201.

———. 1998. Species-range size distributions: products of speciation, extinction and transformation. Philosophical Transactions of the Royal Society B 353:219–230.

———. 2008. Biodiversity and extinction: the dynamics of geographic range size. Progress in Physical Geography 32:678–683.

Gaston, K. J., and R. A. Fuller. 2009. The sizes of species' geographic ranges. Journal of Applied Ecology 46:1–9.

Gaston, K. J., and J. I. Spicer. 2001. The relationship between range size and niche breadth: a test using five species of *Gammarus* (Amphipoda). Global Ecology and Biogeography 10:178–188.

Goldberg, E. E., L. T. Lancaster, and R. H. Rhee. 2011. Phylogenetic inference of reciprocal effects between geographic range evolution and diversification. Systematic Biology 604:451–465.

Harnik, P. G., C. Simpson, and J. L. Payne. 2012. Long-term differences in extinction risk among the seven forms of rarity. Proceedings of the Royal Society B 279:4969–4976.

Heckel, P. H. 1986. Sea-level curve for Pennsylvanian eustatic marine transgressive-regressive depositional cycles along midcontinent outcrop belt, North America. Geology 14:330–334.

Heim, N. A., and S. E. Peters. 2011. Regional environmental breadth predicts geographic range and longevity in fossil marine genera. PLoS ONE 6:e18946.

Hendricks, J. R., B. S. Lieberman, and A. L. Stigall. 2008. Using GIS to study palaeobiogeographic and macroevolutionary patterns in soft-bodied Cambrian arthropods. Palaeogeography, Palaeoclimatology, Palaeoecology 264:163–175.

Hendricks, J. R., E. E. Saupe, C. E. Myers, E. J. Hermsen, and W. D. Allmon. 2014. The generification of the fossil record. Paleobiology 40:511–528.

Holland, S. M. 2020. The stratigraphy of mass extinctions and recoveries. Annual Review of Earth and Planetary Sciences 48:75–97.

Holland, S. M., and M. E. Patzkowsky. 2015. The stratigraphy of mass extinction. Palaeontology 58:903–924.

Hull, P. M., S. A. F. Darroch, and D. H. Erwin. 2015. Rarity in mass extinctions and the future of ecosystems. Nature 528:345–351.

Jablonski, D. 1986. Background and mass extinctions: the alternation of macroevolutionary regimes. Science 231:129–133.

———. 2005. Mass extinctions and macroevolution. Paleobiology 31:192–210.

———. 2008. Extinction and the spatial dynamics of biodiversity. Proceedings of the National Academy of Sciences of the USA 105:11528–11535.

Jablonski, D., and K. Roy. 2003. Geographic range and speciation in fossil and living molluscs. Proceedings of the Royal Society B 270:401–406.

Jones, K. E., A. Purvis, and J. L. Gittleman. 2003. Biological correlates of extinction risk in bats. American Naturalist 161:601–614.

Kocsis, A. T., C. J. Reddin, and W. Kiessling. 2018. The biogeographical imprint of mass extinctions. Proceedings of the Royal Society B 285:20180232.

Kröger, B. 2018. Changes in the latitudinal diversity gradient during the Great Ordovician Biodiversification Event. Geology 46:127–130.

Lester, S. E., B. I. Ruttenberg, S. D. Gaines, and B. P. Kinlan. 2007. The relationship between dispersal ability and geographic range size. Ecology Letters 10:745–758.

Lieberman, B. S. 2004. Range expansion, extinction, and biogeographic congruence: a deep time perspective. Pages 11–124 *in* Frontiers in biogeography: new directions in the geography of nature. M. V. Lomolino and L. R. Heaney, eds. Annals of the Missouri Botanical Garden 222. Sunderland, MA: Sinauer.

Lyons, S. K., P. J. Wagner, and K. Dzikiewicz. 2010. Ecological correlates of range shifts of Late Pleistocene mammals. Philosophical Transactions of the Royal Society B 365:3681–3693.

Macpherson, E. 2003. Species range size distributions for some marine taxa in the Atlantic Ocean: effect of latitude and depth. Biological Journal of the Linnean Society 80:437–455.

Myers, C. E., and B. S. Lieberman. 2010. Sharks that pass in the night: using geographical information systems to investigate competition in the Cretaceous Western Interior Seaway. Proceedings of the Royal Society B 278:681–689.

Noto, C. R. 2010. Hierarchical control of terrestrial vertebrate taphonomy over space and time: discussion of mechanisms and implications for vertebrate paleobiology. Pages 287–336 *in* Taphonomy: process and bias through time. P. A. Allison, and D. J. Bottjer, eds. Topics in Geobiology 32. Springer, Dordrecht.

Nurnberg, S., and M. Aberhan. 2013. Habitat breadth and geographic range predict diversity dynamics in marine Mesozoic bivalves. Paleobiology 39:360–372.

Payne, J. L., and S. Finnegan. 2007. The effect of geographic range on extinction risk during background and mass extinction. Proceedings of the National Academy of Sciences of the USA 104:10506–10511.

Plotnick, R. E. F. 2017. Recurrent hierarchical patterns and the fractal distribution of fossil localities. Geology 45:295–298.

R Core Team. 2019. R: a language and environment for statistical computing. R Foundation for Statistical Computing, Vienna. https://www.R-project.org/.

Raia, P., F. Passaro, D. Fulgione, and F. Carotenuto. 2012. Habitat tracking, stasis, and survival in Neogene large mammals. Biology Letters 8:64–66.

Runge, C. A., A. Tulloch, E. Hammill, H. P. Possingham, and R. A. Fuller. 2015. Geographic range size and extinction risk assessment in nomadic species. Conservation Biology 29:865–876.

Saupe, E. E., H. Qiao, J. R. Hendricks, R. W. Portell, S. J. Hunter, J. Soberon, and B. S. Lieberman. 2015. Niche breadth and geographic range size as determinants of species survival on geological time scales. Global Ecology and Biogeography 24:1159–1169.

Stigall, A. L. 2012. Speciation collapse and invasive species dynamics during the Late Devonian "Mass Extinction." Geological Society of America Bulletin 22:4–9.

Stigall, A. L., and B. S. Lieberman. 2006. Quantitative paleobiogeography: GIS, phylogenetic biogeographic analysis, and conservation insights. Journal of Biogeography 33:2051–2060.

Thuiller, W., S. Lavorel, M. B. Araújo, M. T. Sykes, and I. C. Prentice. 2005. Climate change threats to plant diversity in Europe. Proceedings of the National Academy of Sciences of the USA 102:8245–8250.

Tomašových, A., J. D. Kennedy, T. J. Betzner, N. B. Kuehnle, S. Edie, S. Kim, K. Supriya, A. E. White, C. Rahbek, S. Huang, T. D. Price, and D. Jablonski. 2016. Unifying latitudinal gradients in range size and richness across marine and terrestrial systems. Proceedings of the Royal Society B 283:20153027.

Willis, J. C. 1922. Age and area. Cambridge University Press, Cambridge.

Stratigraphic References

Abbott, M. M. 1998. Freshwater resources and saline water near the Sac and Fox Nation tribal lands, eastern Lincoln County, Oklahoma. US Department of the Interior, US Geological Survey.

Barnes, V. E. 1967. Geologic atlas of Texas, Sherman Sheet; Walter Scott Adkins memorial edition: University of Texas–Austin, Bureau of Economic Geology, 1 sheet, scale 1 : 250,000.

———. 1987. Geologic atlas of Texas, Wichita Falls-Lawton Sheet; Alfred Sherwood Romer memorial edition: University of Texas–Austin, Bureau of Economic Geology, 1 sheet, scale 1 : 250,000.

Bennison, A. P. 1972. Pennsylvanian rocks of the Tulsa area: Seminole Formation.

Bennison, A. P., D. R. Boardman, and L. W. Watney. 1996. Unconformities, hiatuses and paleosols in Midcontinent sequences.

Bloomer, R., E. Harrison, E. Hughes, and D. G. Morris. 1991. Cyclic deposition of Pennsylvanian and Permian sediments of the Eastern Shelf, Texas.

Blumenthal, M. 1958. Subsuface geology of the Prague-Paden area Lincoln and Okfuskee Counties, Oklahoma.

Boardman, D. R., II, M. K. Nestell, and L. W. Knox. 1995. Depth-related microfaunal biofacies model for late Carboniferous and Early Permian cyclothemic sedimentary sequences in Mid-Continent North America.

Bradshaw, S. E., and J. Mazzullo. 1996. Depositional facies and environments of the lower Mineral Wells formation, Pennsylvanian Strawn group, north central Texas.

Branson, C. C. 1962. Pennsylvanian system of the Mid-Continent.

Brister, B. S., W. C. Stephens, and G. A. Norman 2002. Structure, stratigraphy, and hydrocarbon system of a Pennsylvanian pull-apart basin in north-central Texas. AAPG Bulletin 86:1–20.

Brown, S. L. 1967. Stratigraphy and depositional environment of the Elgin Sandstone (Pennsylvanian) in south-central Kansas. University of Kansas.

Cemen, I., A. Sagnak, and S. Akthar. 2002. Geometry of the triangle zone and duplex structure in the Wilburton Gas Field area of the Arkoma basin, southeastern Oklahoma.

Chen, R., and R. W. Scott. 2012. Sedimentology of the Upper Pennsylvanian Bigheart Sandstone Member, Tallant Formation, Pawnee and Osage Counties, Oklahoma.

Cheney, M. G. 1940. Geology of north-central Texas. American Association of Petroleum Geologists Bulletin 24:65–118.

Clark, S. H. B., G. T. Spanski, D. G. Hadley, and A. H. Hofstra. 1993. Geology and mineral resource potential of the Chattanooga 1 degrees × 2 degrees quadrangle, Tennessee and North Carolina; a preliminary assessment. US Geological Survey Bulletin, 2005.

Cleaves, A. W. 1993. Sequence stratigraphy, systems tracts, and mapping strategies for the subsurface Middle and Upper Pennsylvanian of the Eastern Shelf, north-central Texas.

Cocke, J. M., and J. Molinary. 1973. *Dibunophyllum* and *Neokoninckophyllum* from the Wann Formation (Missourian) in northeastern Oklahoma. Journal of Paleontology 47:657–662.

Conselman, F. B. 1961. First day; Brown County road log. Abilene Geological Society Field Trip Guidebook, pp. 9–20.

Cromwell, D. W. 1976. The stratigraphy and environment of deposition of the Lower Dornick Hills Group (Lower Pennsylvanian), Ardmore Basin, Oklahoma.

Cronoble, W. R. 1962. Facies relationships in and adjacent to limestone buildups of the Coffeyville and Hogshooter Formations (Missourian), Washington and Nowata Counties, Oklahoma.

Crosby, E. J., and W. J. Mapel. 1975. Central and west Texas. Pages 197–232 *in* Paleotectonic investigations of the Pennsylvanian System in the United States: part 1, introduction and regional analyses of the Pennsylvanian System. US Geological Survey Professional Paper 853-K.

Davidson, J. D. 1982. Physical stratigraphy of the Avant Limestone Member of the Iola Formation (Missourian), southern Osage County and adjoining counties, Oklahoma.

Denison, R. E., R. B. Koepnick, W. H. Burke, E. A. Hetherington, and A. Fletcher. 1994. Construction of the Mississippian, Pennsylvanian and Permian seawater $^{87}Sr^{86}Sr$ curve. Chemical Geology 112:145–167.

Dogan, N. 1970. Subsurface study of Pennsylvanian rocks in east central Oklahoma (from the Brown Limestone to the Checkerboard Limestone).

Dunn, M. T., G. Mapes, and G. W. Rothwell. 2002. On Paleozoic plants from marine strata: *Hexaloba finisensia* new genus and species, a trigonocarpalean ovule from the Virgilian (Upper Pennsylvanian: Gzhelian) Finis Shale of Texas. Journal of Paleontology 76:173–180.

Dutton, S. P., E. M. Kim, R. F. Broadhead, and W. Raatz. 2003. Play analysis and digital portfolio of major oil reservoirs in the Permian Basin: application and transfer of advanced geological and engineering technologies for incremental production opportunities. Report of Investigations, University of Texas Bureau of Economic Geology, 271.

Dutton, S. P., E. M. Kim, R. F. Broadhead, W. D. Raatz, C. L. Breton, S. C. Ruppel, and C. Kerans. 2005. Play analysis and leading-edge oil-reservoir development methods in the Permian Basin: increased recovery through advanced technologies. AAPG Bulletin 89:553–576.

Dye, J. J. 2010. Analysis of source area evolution through petrologic examination of sandstone, Casper Formation, southeastern WY, USA. *In* 2010 GSA Denver Annual Meeting.

Eargle, D. H. 1960. Stratigraphy of Pennsylvanian and Lower Permian rocks in Brown and Coleman Counties, Texas. Pages D55–D77 *in* P. T. Stafford and others, eds. Pennsylvanian and Lower Permian rocks of parts of west and central Texas. US Geological Survey Professional Paper 315-D.

Eberli, G. P., J. L. Masaferro, and J. F. R. Sarg. 2004. Seismic imaging of carbonate reservoirs and systems. AAPG Memoir 81:107–122.

Elmore, R. D., P. K. Sutherland, and P. B. White. 1990. Middle Pennsylvanian recurrent uplift of the Ouachita fold belt and basin subsidence in the Arkoma basin, Oklahoma. Geology 18:906–909.

Erlich, R. N., and J. L. Coleman Jr. 2005. Drowning of the Upper Marble Falls carbonate platform (Pennsylvanian), central Texas: a case of conflicting "signals"? Sedimentary Geology 175:479–499.

Esquivel-Macías, C., W. I. Ausich, B. E. Buitrón-Sanchez, and A. Flores De Dios. 2000. Pennsylvanian and Mississippian pluricolumnal assemblages (Class Crinoidea) from southern Mexico and a new occurrence of a column with a tetralobate lumen. Journal of Paleontology 74:1187–1190.

Ewing, T. E. 2006. Mississippian Barnett Shale, Fort Worth basin, north-central Texas: gas-shale play with multi–trillion cubic foot potential: discussion. AAPG Bulletin 90:963–966.

Fambrough, J. W. 1964. Isopach and lithofacies study of Virgilian and Missourian series of north-central Oklahoma.

Farrar, K. M., and J. A. Breyer. 2011. Stratigraphy of the Marble Falls Interval (Pennsylvanian), Jack and Wise Counties, Texas.

Fay, R. O. 1997. Stratigraphic units in Oklahoma, Texas, Arkansas, and adjacent areas. Open-File Report 2-97, Oklahoma Geological Survey.

Fisher, M. K., C. A. Wright, B. M. Davidson, N. P. Steinsberger, W. S. Buckler, A. Goodwin, and E. O. Fielder. 2005. Integrating fracture mapping technologies to improve stimulations in the Barnett Shale. SPE Production and Facilities 20:85–93.

Frey, R. C. 1995. Middle and Upper Ordovician nautiloid cephalopods of the Cincinnati arch region of Kentucky, Indiana, and Ohio. Pages P1–P126 *in* J. Pojeta Jr., ed. Contributions to the Ordovician paleontology of Kentucky and nearby states. US Geological Survey Professional Paper 1066-P.

Frost, C. D., and B. R. Frost. 1995. Open-system dehydration of amphibolite, Morton Pass, Wyoming: elemental and Nd and Sr isotopic effects. Journal of Geology 103:269–284.

Furlow, B. 1967. Subsurface geology of the Kellyville District Creek County Oklahoma.

Galloway, W. E., M. S. Yancey, and A. P. Whipple. 1977. Seismic stratigraphic model of depositional platform margin, eastern Anadarko Basin, Oklahoma. AAPG Bulletin 61:1437–47.

Garrouch, A. A., L. Ali, and F. Qasem. 2001. Using diffusion and electrical measurements to assess tortuosity of porous media. Industrial and Engineering Chemistry Research 40:4363–4369.

Grant, J. A., and B. R. Frost. 1990. Contact metamorphism and partial melting of pelitic rocks in the aureole of the Laramie anorthosite complex, Morton Pass, Wyoming. American Journal of Science 290:425–472.

Grayson, R. C., Jr. 1988. Middle and late Pennsylvanian rocks, north-central Texas. South-Central Section of the Geological Society of America, 4, 317.

Groves, J. R. 1983. Calcareous foraminifers and algae from the type Morrowan (Lower Pennsylvanian) region of northeastern Oklahoma and northwestern Arkansas, 133. University of Oklahoma.

———. 1991. Fusulinacean biostratigraphy of the Marble Falls Limestone (Pennsylvanian), western Llano region, central Texas. Journal of Foraminiferal Research 21:67–95.

———. 2000. Suborder Lagenina and other smaller foraminifers from uppermost Pennsylvanian–lower Permian rocks of Kansas and Oklahoma. Micropaleontology 46:285–326.

Guevara, E. H., C. Breton, and P. C. Hackley. 2007. Coal rank and stratigraphy of Pennsylvanian coal and coaly shale samples, Young County, north-central Texas.

Gupta, S. 1970. Miospores from the Desmoinesian-Missourian boundary formations of Texas and the age of the Salesville Formation. Geoscience and Man 1:67–82.

Hackley, P. C., E. H. Guevara, T. F. Hentz, and R. W. Hook. 2009. Thermal maturity and organic composition of Pennsylvanian coals and carbonaceous shales, north-central Texas: implications for coalbed gas potential. International Journal of Coal Geology 77:294–309.

Harlton, B. H. 1956. West Velma oil field. Pages 221–233 *in* Petroleum geology of southern Oklahoma; a symposium. Vol. 1. American Association of Petroleum Geologists Special Volume, no. 16. Prepared in conjunction with the Ardmore Geological Society.

Harrison, E., and D. Mauldin. 2008. Cyclic deposition of Pennsylvanian and Permian sediments on the Eastern Shelf, Texas.

Harrison, E., J. Webster, P. James, C. Easley, and J. Raney. 1999. Stratigraphy of the Colorado and Brazos river basins.

Hentz, T. F. 1988. Lithostratigraphy and paleoenvironments of Upper Palaeozoic Continental Red Beds, north-central Texas: Bowie (new) and Wichita (revised) Groups. Bureau of Economic Geology, University of Texas at Austin, Report of Investigations, 170.

Heran, W. D., G. N. Green, and D. B. Stoeser. 2003. a Alluvium, Q., al Alluvium, Q., d Dune Sand, Q., . . . and b Basalt, T. US Department of the Interior US Geological Survey Open File Report 03-247. Version 1.0 A digital geologic map database for the state of Oklahoma.

Hinds, H., F. C. Greene, and D. White. 1915. The stratigraphy of the Pennsylvanian Series in Missouri. Vol. 13. H. Stephens.

Hoare, R. D., R. H. Mapes, and T. E. Yancey. 2002. Structure, taxonomy, and epifauna of Pennsylvanian rostroconchs (Mollusca). Journal of Paleontology 76:1–30.

Hoare, R. D., M. T. Sturgeon, and T. B. Hoare. 1972. Middle Pennsylvanian (Allegheny Group) polyplacophora from Ohio. Journal of Paleontology 46:675–680.

Holland, S. M., and M. E. Patzkowsky. 1998. Sequence stratigraphy and relative sea-level history of the Middle and Upper Ordovician of the Nashville Dome, Tennessee. Journal of Sedimentary Research 68:684–699.

Holmes, R., D. S. Berman, and J. S. Anderson. 2013. A new dissorophid (Temnospondyli, Dissorophoidea) from the Early Permian of New Mexico (United States). Comptes Rendus Palevol 12:419–435.

Hughes, E. N. 2011. Chemostratigraphy and paleoenvironment of the Smithwick Formation, Fort Worth Basin, San Saba County, Texas.

Jarvie, D. M., R. J. Hill, T. E. Ruble, and R. M. Pollastro. 2007. Unconventional shale-gas systems: the Mississippian Barnett Shale of north-central Texas as one model for thermogenic shale-gas assessment. AAPG bulletin 91:475–499.

Kerr, D. R., L. S. Ye, A. Bahar, B. M. Kelkar, and S. L. Montgomery. 1999. Glenn Pool field, Oklahoma: a case of improved production from a mature reservoir. AAPG Bulletin 83:1–18.

Kerr, S. D., Jr. 1969. Algal-bearing carbonate reservoirs of Pennsylvanian age, West Texas and New Mexico: abstract. AAPG Bulletin 53:726–727.

Kissel, R. A., Jr. 1999. Paleontology and geology of an Upper Pennsylvanian tetrapod locality from the Ada Formation, Seminole County, Oklahoma. PhD diss. Texas Tech University.

Krumme, G. W. 1981. Stratigraphic significance of limestones of the Marmaton Group (Pennsylvanian, Desmoinesian) in eastern Oklahoma. University of Oklahoma.

Lang, R. C. 1966. First day of the field trip: the Pennsylvanian rocks of the Lake Murray area.

Lee, B. E. 1982. Stratigraphy, sedimentology and uranium potential of Virgilian-Leonardian strata of the Hollis-Hardeman Basin, Oklahoma and Texas.

Lin, R., and W. W. Nassichuk. 1994. Fusulinaceans at the Middle/Upper Pennsylvanian (Desmoinesian/Missourian) boundary in the Canadian Arctic Archipelago.

Lobza, V., J. Schieber, and M. Nestell. 1994. The influence of sea level changes and possible pycnocline shifts on benthic communities in the Finis Shale (Virgilian) near Jacksboro, north-central Texas.

Lojek, C. A. 1985. Petrology, diagenesis and depositional environment of the Skinner sandstones, Desmoinesian Northeast Oklahoma Platform.

Long, J. S. 1997. Regression models for categorical and limited dependent variables. Sage, Thousand Oaks, CA.

Lucas, S. G. 2006. Global Permian tetrapod biostratigraphy and biochronology. Geological Society Special Publications 265:65–93.

Lucas, S. G., and A. J. Lerner. 2001. Reappraisal of Oklahomaichnus, a supposed amphibian trackway from the Pennsylvanian of Oklahoma, USA.

Lyday, J. R. 1985. Atokan (Pennsylvanian) Berlin field: genesis of recycled detrital dolomite reservoir, deep Anadarko Basin, Oklahoma. AAPG Bulletin 69:1931–1949.

Mazzullo, S. J., D. R. Boardman, E. L. Grossman, and K. Dimmick-Wells. 2007. Oxygen-carbon isotope stratigraphy of upper Carboniferous to lower Permian marine deposits in Midcontinent USA (Kansas and NE Oklahoma): implications for sea water chemistry and depositional cyclicity. Carbonates and Evaporites 22:55–72.

McBride, M. H., P. C. Franks, and R. E. Larese. 1987. Chlorite grain coats and preservation of primary porosity in deeply buried Springer Formation and Lower Morrowan Sandstones, southeastern Anadarko Basin, Oklahoma. AAPG Bulletin 71:994.

Meagher, B. E. 2012. Microfaunal assemblages of the Placid Shale (Missourian, Upper Pennsylvanian), Brazos River valley, North-Central Texas.

Merrill, G. K., and P. H. Von Bitter. 2007. The Pennsylvanian conodont genus Gondolella Stauffer and Plummer, 1932: reinterpretation of

the original type specimens and concepts. Journal of Micropalaeontology 26:41–46.

Mii, H. S., E. L. Grossman, and T. E. Yancey. 1999. Carboniferous isotope stratigraphies of North America: implications for Carboniferous paleoceanography and Mississippian glaciation. Geological Society of America Bulletin 111:960–973.

Montgomery, S. L., D. M. Jarvie, K. A. Bowker, and R. M. Pollastro. 2005. Mississippian Barnett Shale, Fort Worth Basin, north-central Texas: gas-shale play with multi–trillion cubic foot potential. AAPG Bulletin 89:155–175.

Myers, D. A. 1960. Stratigraphic distribution of some Pennsylvanian Fusulinidae from Brown and Coleman Counties, Texas. US Government Printing Office.

———. 1966. *Oketaella earglei*, a new fusulinid species, from the Adams Branch Limestone Member of the Graford Formation of Late Pennsylvanian age, Brown County, Texas. Geological Survey Professional Paper 550, 47.

Northcutt, R. A. 2002. History of Hunton oil and gas exploration and development in Oklahoma.

Nützel, A., D. H. Erwin, and R. H. Mapes. 2000. Identity and phylogeny of the late Paleozoic Subulitoidea (Gastropoda). Journal of Paleontology 74:575–598.

Oakes, M. C. 1951. The proposed Barnsdall and Tallant formations in Oklahoma. Tulsa Geological Society Digest 19:119–122.

Petty, A. J., Jr. 1975. Biostratigraphy of the Graford Formation, Missourian, Wise County, Texas. PhD diss. University of Texas at El Paso.

Plummer, F. B. 1919. Preliminary paper on the stratigraphy of the Pennsylvanian formations of north-central Texas, with discussion. American Association of Petroleum Geologists Bulletin 3:132–150.

Plummer, F. B., and R. C. Moore. 1922. Stratigraphy of the Pennsylvanian formations of north-central Texas. University of Texas Bulletin no. 2132.

Pollastro, R. M., R. J. Hill, D. M. Jarvie, and M. E. Henry. 2003. Assessing undiscovered resources of the Barnett-Paleozoic total petroleum system, Bend Arch-Fort Worth Basin province, Texas.

Pollastro, R. M., D. M. Jarvie, R. J. Hill, and C. W. Adams. 2007. Geologic framework of the Mississippian Barnett Shale, Barnett-Paleozoic total petroleum system, Bend arch—Fort Worth Basin, Texas. AAPG Bulletin 91:405–436.

Pybas, G. W. 1964. Petroleum geology of southwestern Pottawatomie County, Oklahoma.

Ross, C. S. 1921. The Lacasa area, Ranger district, north-central Texas. Pages 303–314 *in* Contributions to economic geology, 1921: part 2, mineral fuels. US Geological Survey Bulletin 726-G.

Rosscoe, S. J. 2008. *Idiognathodus* and *Streptognathodus* species from the lost branch to Dewey sequences (middle-upper Pennsylvanian) of the midcontinent basin, North America. PhD diss. Texas Tech University.

Sadd, J. L. 1991. Tectonic influences on carbonate deposition and diagenesis, Buckhorn Asphalt, Deese Group (Desmoinesian), Arbuckle Mountains, Oklahoma. Journal of Sedimentary Research 61:28–42.

Schieber, J. 2011. Marcasite in black shales—a mineral proxy for oxygenated bottom waters and intermittent oxidation of carbonaceous muds. Journal of Sedimentary Research 81:447–445.

Seale, J. D. 1982. Depositional environments and diagenesis of Upper Pennsylvanian Marchand Sandstones on south, east and northeast flanks of the Anadarko Basin.

Sellards, E. H. 1932. The pre-Paleozoic and Paleozoic systems in Texas, part 1. Pages 15–238 *in* E. H. Sellards, W. S. Adkins, and F. B. Plummer. The geology of Texas. Vol. 1. Stratigraphy. University of Texas Bulletin no. 3232.

Shelton, J. W. 1981. Guidebook to depositional environments of selected Pennsylvanian sandstones of northeastern Oklahoma, 1981.

Shelton, J. W., and T. L. Rowland. 1974. Guidebook to the depositional environments of selected Pennsylvanian sandstones and carbonates of Oklahoma. Geological Society of America, South-Central Section.

Strimple, H. L., and C. Pareyn. 1982. *Cibolocrinus* from the Namurian of North Africa with notes on the genus. Journal of Paleontology 56:226–232.

Summervill, M. R., and W. Yang. 2003. Regional subsurface study of the oread cyclothem in south-central Kansas—a preliminary investigation.

Sumrall, C. D., and A. L. Bowsher. 1996. *Giganticlavus*, a new genus of Pennsylvanian edrioasteroid from North America. Journal of Paleontology 70:986–993.

Suneson, N. H. 1998. Geology of the Hartshorne Formation, Arkoma Basin, Oklahoma. Guidebook 31, Oklahoma Geological Survey.

Sutherland, P. K. 1988. Late Mississippian and Pennsylvanian depositional history in the Arkoma Basin area, Oklahoma and Arkansas. Geological Society of America Bulletin 100:1787–1802.

Sutherland, P. K., B. E. Archinal, and R. K. Grubbs. 1982. Morrowan and Atokan (Pennsylvanian) stratigraphy in the Arbuckle Mountains area, Oklahoma: Lower and Middle Pennsylvanian stratigraphy in south-central Oklahoma. Oklahoma Geological Survey Guidebook 20.

Thomka, J. R., R. D. Lewis, D. Mosher, R. K. Pabian, and P. F. Holterhoff. 2011. Genus-level taphonomic variation within cladid crinoids from the Upper Pennsylvanian Barnsdall Formation, northeastern Oklahoma. Palaios 26:377–389.

Tomlinson, C. W., and W. McBee Jr. 1962. Pennsylvanian sediments and orogenies of Ardmore district, Oklahoma.

Wahlman, G. P., and R. R. West. 2011. Fusulinids from the Howe Limestone Member (Red Eagle Limestone, Council Grove Group) in northeastern Kansas and their significance to the North American Carboniferous (Pennsylvanian)–Permian boundary. Current Research in Earth Sciences Bulletin 258:1–13.

Wardlaw, B. R. 2004. Building an international Permian System and its correlation in the USA. Geological Society of America Abstracts with Programs 36:67.

Wardlaw, B. R., and V. I. Davydov. 2000. Preliminary placement of the international Lower Permian working standard to the Glass Mountains, Texas. International Commission on Stratigraphy International Union of Geological Sciences 11.

Webb, G. E., and J. E. Sorauf. 2002. Zigzag microstructure in rugose corals: a possible indicator of relative seawater Mg/Ca ratios. Geology 30:415–418.

Whitaker, A. E., and T. Engelder. 2006. Plate-scale stress fields driving the tectonic evolution of the central Ouachita salient, Oklahoma and Arkansas. Geological Society of America Bulletin 118:710–723.

Wilson, C. W., Jr. 1935. Age and correlation of Pennsylvanian surface formations, and of oil and gas sands of Muskogee County, Oklahoma. American Association of Petroleum Geologists Bulletin 19:503–520.

Wilson, L. R. 1966. Palynological evidence for Mississippian Age of the Springer Formation. Pages 20–24 *in* Pennsylvanian of the Ardmore Basin, Southern Oklahoma. American Association of Petroleum Geologists.

———. 1984. Evidence for a new Desmoinesian-Missourian boundary (Middle Pennsylvanian) in Tulsa County, Oklahoma, USA. Pages 251–265 *in* Evolutionary botany and biostratigraphy. A. K. Ghosh commemoration volume. Current Trends in Life Sciences 10. Today and Tomorrow's, New Delhi.

Work, D. M., and R. H. Mapes. 2009. New occurrences of the Pennsylvanian Index Ammonoid Dunbarites from the North American Midcontinent. Journal of Paleontology 83:405–413.

Workman, J. B., and W. A. Braddock. 2010. Geologic map of the Sand Creek Pass Quadrangle, Larimer County, Colorado, and Albany County, Wyoming. US Department of the Interior, US Geological Survey.

Wright, W. R. 2011. Pennsylvanian paleodepositional evolution of the greater Permian Basin, Texas and New Mexico: depositional systems and hydrocarbon reservoir analysis. AAPG Bulletin 95:1525–1555.

Yancey, T. E., and A. W. Cleaves. 1990. Carbonate and siliciclastic sedimentation in Late Pennsylvanian cycles, north-central Texas.

Yang, W. 1996. Cycle symmetry and its causes, Cisco group (Virgilian and Wolfcampian), Texas. Journal of Sedimentary Research 66:1102–1121.

Yang, W., and M. A. Kominz. 2003. Characteristics, stratigraphic architecture, and time framework of multi-order mixed siliciclastic and carbonate depositional sequences, outcropping Cisco Group (Late Pennsylvanian and Early Permian), Eastern Shelf, north-central Texas, USA. Sedimentary Geology 154:53–87.

Associate Editor: Daniel L. Rabosky
Editor: Jennifer A. Lau

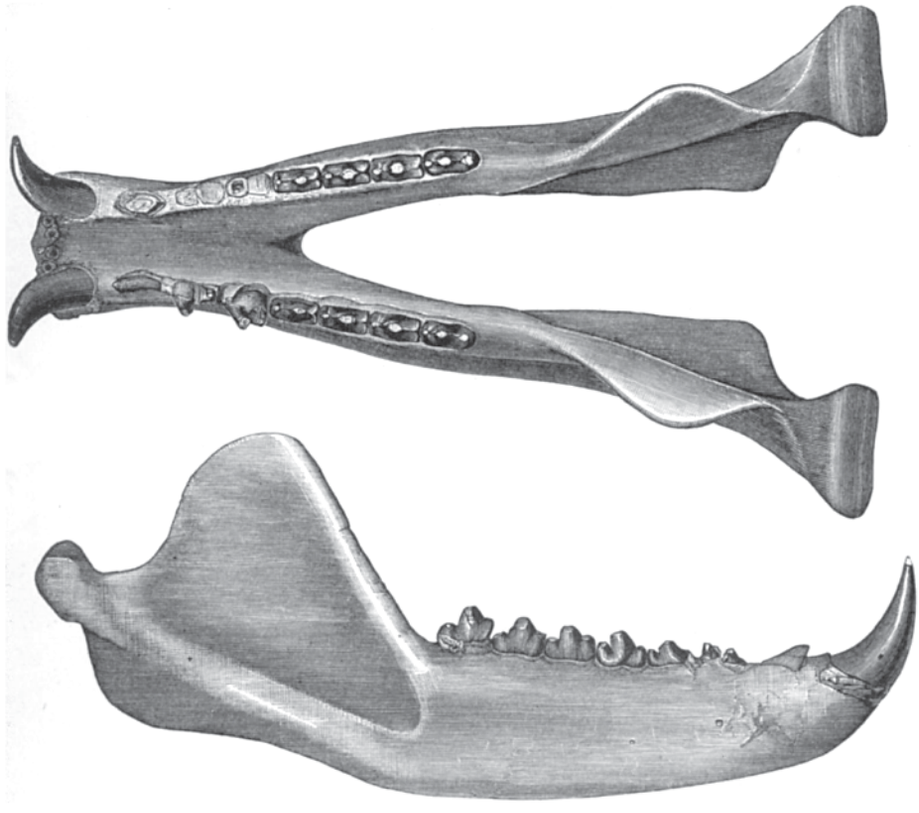

"The *Mesonyx ossifragus* is the largest species, its skull exceeding that of the grizzly bear in dimensions. . . . The fore limbs are so much shorter than the hind limbs that the animal customarily sat on its haunches when on land. In walking, its high rump and low withers would give it somewhat the figure of a huge rabbit." Figured: "Mandible of *Mesonyx ossifragus* Cope, from the Wasatch epoch of the Big Horn river, Wyoming." From "The Creodonta" by E. D. Cope (*The American Naturalist*, 1884, 18:255–267).